Biochimica et Biophysica Acta, 1057 (1991) 51–63

ADONIS 000527289100076W

BBABIO 43350

Reduction of the Q-pool by duroquinol via the two quinone-binding sites of the QH_2 : cytochrome *c* oxidoreductase. A model for the equilibrium between cytochrome *b*-562 and the Q-pool

Carla A.M. Marres and Simon de Vries

Department of Cellular Biology, Section for Molecular Biology and E.C. Slater Institute for Biochemical Research, University of Amsterdam, Amsterdam (The Netherlands)

(Received 29 May 1990)

Key words: Mitochondrion; QH_2 : cytochrome *c* oxidoreductase; Cytochrome bc_1 complex; Ubiquinone; Respiratory chain

The steady-state reduction of exogenous ubiquinone-2 by duroquinol as catalysed by the ubiquinol : cytochrome *c* oxidoreductase was studied in bovine heart mitoplasts. The reduction of ubiquinone-2 by duroquinol proceeds both in the absence of inhibitors of the enzyme, in the presence of outside inhibitors, e.g., myoxthiazol, and in the presence of inside inhibitors, e.g., antimycin, but not in the presence of both inside and outside inhibitors. It is concluded that both the Q_{in}-binding domain and the Q_{out}-binding domain may independently catalyse this reaction. The rate of the reduction of ubiquinone-2 by duroquinol via the Q_{in}-binding domain is dependent on the type of outside inhibitor used. The maximal rate obtained for the reduction of ubiquinone-2 by DQH_2 via the Q_{out}-binding domain, measured in the presence of antimycin, is similar to that catalysed by the Q_{in}-binding domain of the non-inhibited enzyme and depends on the redox state of the high-potential electron carriers of the respiratory chain. The reduction of ubiquinone-2 by DQH_2 via the Q_{in}-binding domain can be described by a mechanism in which duroquinol reduces the enzyme, upon which the reduced enzyme is rapidly oxidized by ubiquinone-2 yielding ubiquinol-2. By determination of the initial rate under various conditions and simulation of the time course of reduction of ubiquinone-2 using the integrated form of the steady-state rate equation the values of the various kinetic constants were calculated. During the course of reduction of ubiquinone-2 by duroquinol in the presence of outside inhibitors only cytochrome *b*-562 becomes reduced. At all stages during the reaction, cytochrome *b*-562 is in equilibrium with the redox potential of the ubiquinone-2/ubiquinol-2 couple but not with that of the duroquinone/duroquinol couple. At low pH values, cytochrome *b*-562 is reduced in a single phase; at high pH separate reduction phases are observed. In the absence of inhibitors three reduction phases of cytochrome *b*-562 are discernible at low pH values and two at high pH values. In the presence of antimyin cytochrome *b* becomes reduced in two phases. Cytochrome *b*-562 is reduced in the first phase and cytochrome *b*-566 in the second phase after substantial reduction of ubiquinone-2 to ubiquinol-2 has occurred. In ubiquinone-10 depleted preparations, titration of cytochrome *b*-562, in the presence of myxothiazol, with the duroquinone/duroquinol redox couple yields a value of $n_{app} = 2$, both at low and high pH. In contrast, in ubiquinone-containing preparations, values of n_{app} close to 2 and below 1 were calculated at low and high pH values, respectively. These observations are incorporated in a model describing quantitatively the redox equilibrium between cytochrome *b*-562 and the pool of ubiquinone-2 via the Q_{in}-binding domain. A key feature of the model is that ubiquinol : cytochrome *c* oxidoreductase is present as a dimeric enzyme, each protomer harbouring one heme *b*-562 with the same standard midpoint potential and one Q_{in}-binding domain. According to the model, electron transfer may occur between two quinones bound to the two Q_{in}-binding domains thus allowing redox equilibration between two hemes *b*-562 within the dimeric enzyme. Accordingly, the

Abbreviations: Q, Q^{-}, $Q^{\cdot -}$, QH_2, (ubi)quinone, (ubi)semiquinone anion, (ubi)quinol; Q_2, Q_{10}, ubiquinone-2 and ubiquinone-10; DQ, duroquinone; BAL, British Anti-Lewisite (2,3-dimercaptopropanol).

Correspondence: C.A.M. Marres, Department of Cellular Biology, Section for Molecular Biology, University of Amsterdam, Kruislaan 318, 1098 SM Amsterdam, The Netherlands.

change in the course of reduction of cytochrome *b*-562, in the presence of myxothiazol, from monophasic, at low pH, to biphasic at high pH is due to the increase in the stability (constant) of the antimycin-sensitive semiquinone anion bound to the Q_{in}-binding domain.

Introduction

It is generally recognized that ubiquinone and cytochrome *b* function in the main stream of respiratory and photoredox chains. The low rate of oxidation/reduction of both redox components, previously considered to indicate that they are located only on a side path, was proposed to be due to the large size of the quinone pool and the rapid equilibrium between ubiquinone and cytochrome *b* [1,2]. Although the nature of this rapid equilibrium was not further specified in Ref. 1, we can now, after the proposal of the Q cycle [3] and its experimental verification in great detail (see Refs. 4–9 for reviews), speculate that the antimycin-sensitive equilibrium between quinone bound to the Q_{in}-binding domain and cytochrome *b*-562 is given by the reaction

$$Q_{in} + 2b^{2+}_{562} + 2H^+ \leftrightarrow Q_{in}H_2 + 2b^{3+}_{562} \quad (1)$$

The presence of two different Q-reactive domains in the bc_1 complex complicates the redox behaviour of cytochrome *b*, because it may be reduced via both domains. Indeed, the multiphasic pattern of reduction of cytochrome *b*-562, observed in succinate pulse experiments with mitochondrial enzyme preparations, is due to the oxidation of quinol via the Q_{out}-binding domain, followed by the reduction of cytochrome *b*-562 via the Q_{in}-binding domain, i.e. the reversal of reaction (1), once cytochrome c_1 and the Rieske Fe-S cluster are reduced [10–12]. Although there is disagreement whether real net oxidation of cytochrome *b*-562 occurs after the initial rapid reduction, when succinate is used as the reductant, the kinetics of the multiphasic reduction of cytochrome *b*-562 can be simulated in terms of the Q cycle [13]. When DQH_2 instead of succinate is used as reductant a rapid (partially) antimycin-sensitive reduction of Q_{10} by DQH_2 is observed [14,15], i.e., within 5 ms 1 mol $Q_{10}H_2$ per mol bc_1 complex is formed, whereas from the degree of reduction of cytochrome c_1 and the Fe-S cluster one has to conclude that about 0.5 mol DQH_2 per mol bc_1 complex is oxidized via the Q_{out}-binding domain. Hence, in an experiment in which DQH_2 is employed as reductant, the two Q-reactive domains may be operating simultaneously.

These examples indicate that the actual pattern of reduction of cytochrome *b*-562 is dependent on the type of reductant. In addition, one may conclude from the work presented in Refs. 16–27 that the rate and extent of reduction of cytochrome *b*-562 is also dependent on the size of the Q pool, the pH and the particular bc_1 (*bf*) complex under study. In some of these studies [16,19,20,24,25], it was noticed that the equilibrium between cytochrome *b*-562 and the Q pool is not correctly described by Eqn. 1. In particular, the finding that cytochrome *b*-562 titrates with a value of *n* close to 2 is not given by this reaction equation. We have therefore undertaken a study to describe qualitatively and quantitatively the equilibrium between cytochrome *b*-562 and the Q pool under a variety of experimental conditions.

Material and Methods

Beef-heart mitoplasts freed of cytochrome *c* and Q-extracted particles were prepared as described in Refs. 28 and 29, respectively. The amount of Q_{10} remaining in the particles was determined by HPLC as in Ref. 15 and was lower than 0.01 mol Q/mol bc_1 complex. BAL(+O_2)-treatment was carried out as in [30]. Q_2 was synthesized according to Ref. 31. Q_2H_2 and DQH_2 were prepared freshly by reducing the corresponding quinones, dissolved in Me_2SO + 10% H_2O, with borohydride followed by slight acidification.

Spectrophotometric measurements were performed as described in [14,15,17]. Antimycin, myxothiazol and stigmatellin were dissolved in Me_2SO and the concentrations were determined spectrophotometrically as described in Refs. 32–34. The concentration of Q_2 was determined using $\varepsilon_{276\,nm} = 12.2$ (cm mM)$^{-1}$ and for DQH_2 $\varepsilon_{287\,nm} = 2.6$ (cm mM)$^{-1}$ was used, both in ethanol [35]. The [bc_1 complex] was measured fluorometrically by determination of the antimycin binding sites [36]. The extinction coefficient of cytochrome *b*-562 (562–575 nm) was determined at 37.3 (cm mM)$^{-1}$ by potentiometric titration (cf. Ref. 8), in good agreement with the value of 28–28.5 (cm mM)$^{-1}$ for two cytochromes *b* [37], taking a 2 to 1 spectral contribution for cytochrome *b*-562 and cytochrome *b*-566, respectively, at 563–575 nm [cf. Refs. 38–40]. Myxothiazol did not change the peak-minus-trough difference of cytochrome *b*-562 (at 429–412 nm), nor did it affect the midpoint potential by more than 5 mV (cf. Appendix).

Reduction of Q_2 was measured at the wavelength pair 300–284 nm which is isosbestic for changes in the redox state of the DQH_2/DQ redox couple. Unless stated otherwise, reduction of cytochrome *b*-562 was measured at 429–412 nm (at which wavelength pair the extinction coefficient equals 100 (cm mM)$^{-1}$). All experiments were performed at 2°C to slow down the

kinetics. All buffers contained 0.25 M sucrose, 1 mM EDTA and 50 mM Mops-KOH (pH < 6.5) or 50 mM KP_i.

Results

The QH_2 : cytochrome *c* oxidoreductase catalyses both the steady-state electron transfer from QH_2 to cytochrome *c* and from DQH_2 to endogenous Q_{10} or exogenous Q_2. Fig. 1 shows the time-course of reduction of varying amounts of Q_2 by DQH_2 in cyanide-inhibited particles. The initial rate of reduction of Q_2 by DQH_2 was found to increase with increasing concentrations of DQH_2 and Q_2 and to decrease with increasing concentrations of Q_2H_2 (not shown) in the same way as described for the enzyme from *Neurospora crassa* in Ref. 27. The rate is independent of the DQ concentration in agreement, with Ref. 27. The steady-state rate (expressed in electrons per second) of reduction of Q_2 by DQH_2 in cyanide-inhibited preparations is about equal to that of reduction of cytochrome *c* by DQH_2 under the same experimental conditions (data not shown). In the presence of the two inhibitors myxothiazol and antimycin the reduction of Q_2 by DQH_2 is completely abolished. However, in the presence of either inhibitor reduction of Q_2 by DQH_2 does occur (see below), indicating that the steady-state reduction of Q by DQH_2 is catalyzed by the Q_{in}-reactive site in the presence of Q_{out}-inhibitors and by the Q_{out}-reactive site in the presence of Q_{in}-inhibitors.

Reduction of the Q-pool and cytochrome b in the presence of outside inhibitors

Fig. 2 shows the time-course of reduction of cytochrome *b*-562 by DQH_2 in BAL(+O_2)-treated mitoplasts in the presence of varying, but saturating at the $[DQH_2]$ used, amounts of Q_2. The time required to (completely) reduce cytochrome *b*-562 is proportional to the size of the Q_2 pool. This is also observed in KCN- and myxothiazol-inhibited mitoplasts (not shown). Since during the recording of the traces the DOH_2/DQ ratio is practically constant ($[DQH_2] \gg [Q_2]$) whereas the Q_2H_2/Q_2 ratio changes from 0 to about 100, the redox behaviour of cytochrome *b*-562 is indicative for a rapid equilibrium between cytochrome *b*-562 and the Q_2 pool (and not the 'DQH_2' pool). A rapid equilibrium between cytochrome *b*-562 and the

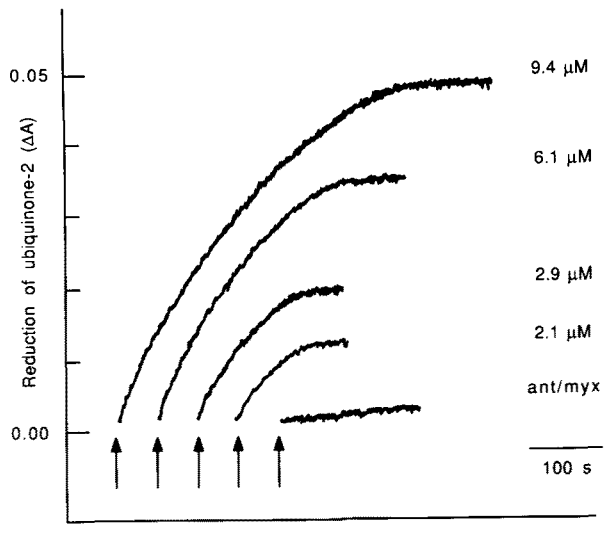

Fig. 1. Kinetics of the reduction of Q_2 by DQH_2 in mitoplasts (76 nM in bc_1 complex) inhibited by KCN (pH 6.2). In the right trace antimycin (ant) and myxothiazol (myx) were added at 3 μM in addition to 9.3 μM Q_2. [KCN] = 1.0 mM. Arrows indicate the addition of 80 μM DQH_2.

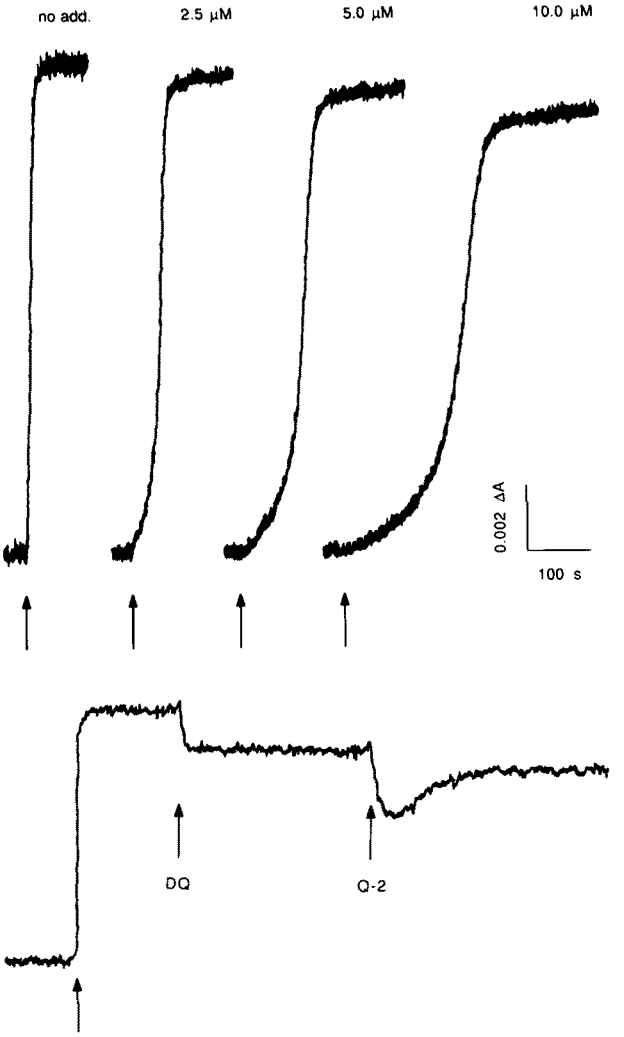

Fig. 2. Kinetics of reduction of cytochrome *b*-562 by DQH_2 in BAL(+O_2)-treated mitoplasts in the presence of different amounts of Q_2 (upper traces). In the lower trace, reduction of cytochrome *b*-562 by DQH_2 is shown (initially, no Q_2 was added) followed by the addition of DQ (75 μM) and Q_2 (10 μM) leading to oxidation and transient oxidation, respectively, of cytochrome *b*-562. The BAL(+O_2)-treated mitoplasts contained 0.05 mol intact Fe-S cluster/mol bc_1 complex. Arrows indicate the addition of DQH_2. Amounts of Q_2 added are indicated above the traces. The amount of endogenous Q_{10} is about 0.7 μM. pH 6.2. [KCN] = 1.0 mM. $[DQH_2]$ = 80 μM in the upper traces and 200 μM in the lower one. [bc_1 complex] = 76 nM (upper) and 40 nM (lower), respectively.

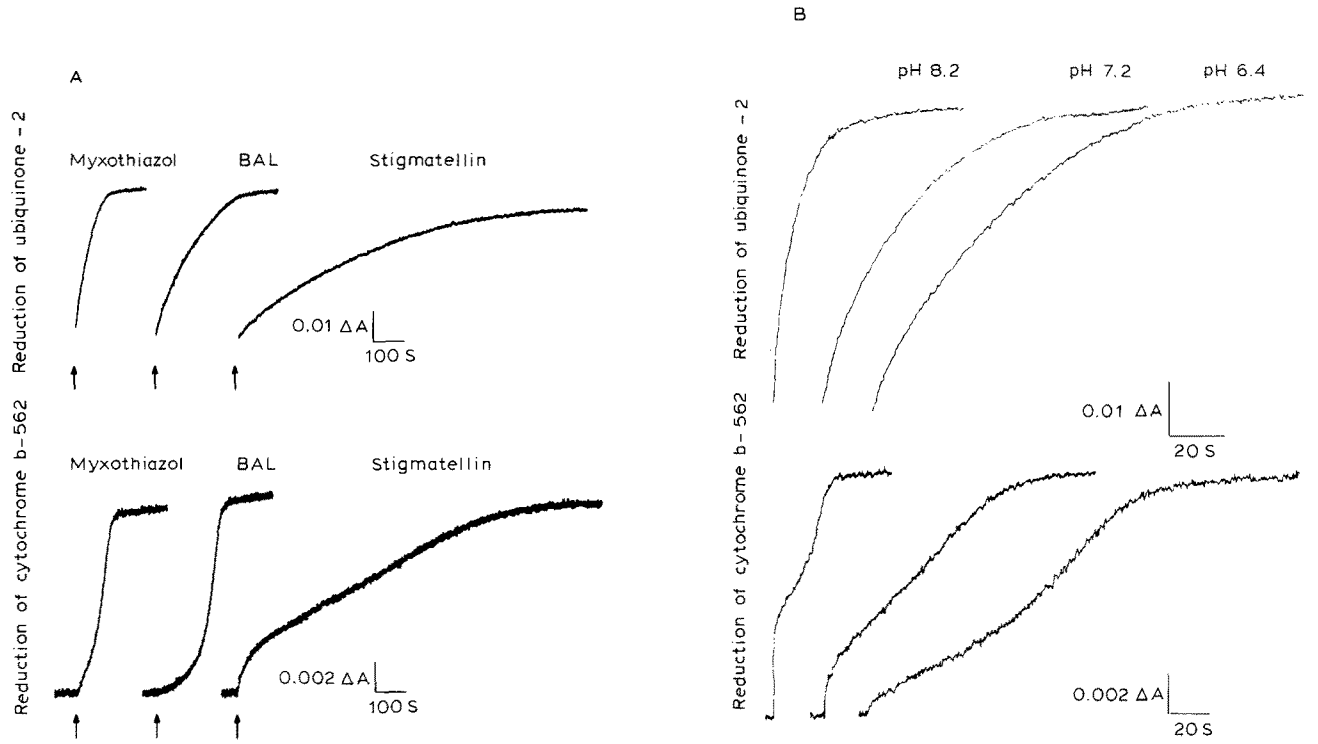

Fig. 3. (A) Time-course of reduction of Q_2 (9.3 μM) by DQH_2 (80 μM) in mitoplasts (76 nM in bc_1 complex) in the presence of various outside inhibitors (upper traces) and reduction of cytochrome *b*-562 under the same experimental conditions (lower traces). pH 6.2; [KCN] = 1.0 mM. (B) Time-course of reduction of Q_2 (upper traces) and cytochrome *b*-562 (lower traces) by DQH_2 in mitoplasts inhibited by myxothiazol (3 μM) at different pH values. [KCN] = 1.0 mM.

Q_2 pool is further illustrated by the lower trace in Fig. 2. The addition of Q_2 to BAL ($+O_2$)-treated particles previously reduced by DQH_2 leads to a transient oxidation of cytochrome *b*-562, i.e., after addition of Q_2, cytochrome *b*-562 is very rapidly oxidized and subsequently slowly reduced, the slow reduction phase corresponding to the reduction of the Q_2 pool by DQH_2. Note, however, that the redox state of cytochrome *b*-562

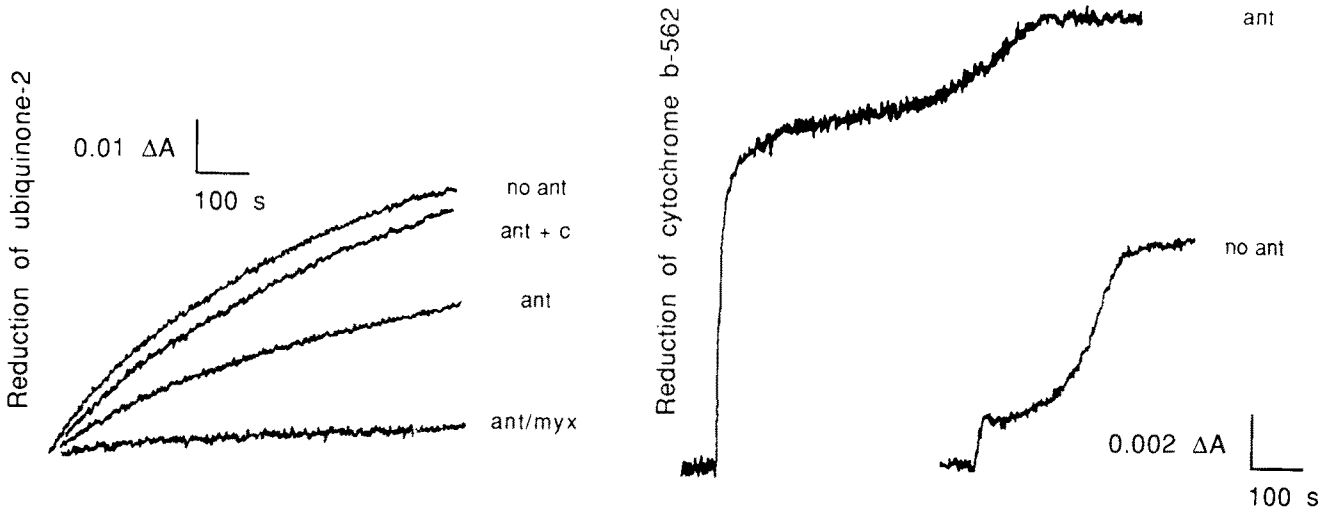

Fig. 4. Time-course of reduction of Q_2 (left) and cytochrome *b*-562 (right) by DQH_2 in mitoplasts inhibited by antimycin (3 μM). The redox state of the Fe-S cluster was manipulated by the addition of ferricytochrome *c* (4 μM) as indicated in the left figure. No add. indicates no addition of antimycin. [bc_1 complex] = 76 nM (left) and 304 nM (right). Cytochrome *b*-562 was monitored at 562–575 nm. For all traces: pH 6.2. [KCN] = 1.0 nM. [DQH_2] = 80 μM. [Q_2] = 10 μM.

may also be affected by the DQH_2/DQ redox couple as indicated by the oxidation of cytochrome *b*-562 after a pulse of DQ.

Fig. 3A shows that the rate of reduction of Q_2 and cytochrome *b*-562 is dependent on the type of outside inhibitor used. The highest rate of reduction of Q_2 is obtained with myxothiazol, the lowest with stigmatellin and an intermediate rate in BAL($+O_2$)-treated mitoplasts, the latter being similar to the rate observed in cyanide-inhibited mitoplasts.

Fig. 3B shows that upon increasing the pH the rate of reduction of the Q_2 pool and of cytochrome *b*-562 increases. It is also seen that the pattern of reduction of cytochrome *b*-562 changes with pH. At pH values below 6.0 the first phase is absent (not shown, but cf. Fig. 2).

Reduction of the Q pool and cytochrome b-562 by DQH_2 in the presence of inside inhibitors

Fig. 4 shows that in the presence of antimycin DQH_2 is able to reduce the Q_2 pool. In contrast to the experiments of Fig. 2, reduction of the Q_2 pool in this case is catalysed by the Q_{out}-binding domain. The rate of reduction of the Q_2 pool in the presence of antimycin is about 2-times lower than that in the presence of KCN only. The rate of the reaction is, however, dependent on the redox state of the high-potential carriers of the respiratory chain. Addition of ascorbate completely inhibited the reaction (not shown), whereas addition of oxidized cytochrome *c* stimulates the rate approximately to that observed in KCN-inhibited mitoplasts. In the presence of antimycin, cytochrome *b* reduced by DQH_2 is transiently oxidized by a pulse of Q_2 (not shown, but cf. Fig. 2). In the presence of a large Q_2 pool the reduction of cytochrome *b* is no longer monophasic but biphasic (Fig. 4) (cf. Refs. 14 and 17). Spectral measurements indicated that cytochrome *b*-562 is reduced in the first phase and cytochrome *b*-566 in the second phase (not shown). These findings indicate that cytochrome *b*-566 rapidly equilibrates with the Q_2 pool. Whether this is a true or a quasi-equilibrium cannot be decided, since the redox state of the [2Fe-2S] cluster is not known under these experimental conditions.

Reduction of the Q pool and cytochrome b-562 in the absence of inhibitors of the bc_1 complex

In the presence of KCN but in the absence of cytochrome bc_1 inhibitors, the reduction of Q_2 by DQH_2 (Fig. 5A) may be due to the catalytic activity of both the Q_{in}- and Q_{out}-binding domain only for the first 1.5 s (i.e., the time required to completely reduce cytochrome c_1 and the Fe-S cluster under the experimental conditions of Fig. 5A) but thereafter only the Q_{in}-reactive domain is active.

It is well known that the course of reduction of cytochrome *b*-562 by DQH_2 or succinate shows multiple reduction phases. After the initial rapid reduction phase, comprising 35–40% of the total absorbance of cytochrome *b*-562 a lag period is observed in which no net reduction of cytochrome *b*-562 takes place and which is followed by a relatively slow reduction phase [10–15]. This pattern of reduction of cytochrome *b*-562 in KCN-inhibited mitoplasts (pH 6.2) is shown in Fig. 5A, left trace. When exogenous Q_2 is added to increase the size of the Q pool the extent of the initial rapid phase decreases. Under these conditions three reduction phases are observed. Furthermore, it is observed that the time required for complete reduction of cytochrome *b*-562 is increased upon increasing the size of the Q-pool so that the lag period (between phase II and phase III) apparently has become longer.

Upon increasing the pH the rate of reduction of the Q_2 pool (not shown) and of cytochrome *b*-562 increases (Fig. 5B) and the lag period between phases II and III apparently decreases. In addition, the extent of the first reduction phase of cytochrome *b*-562 increases with

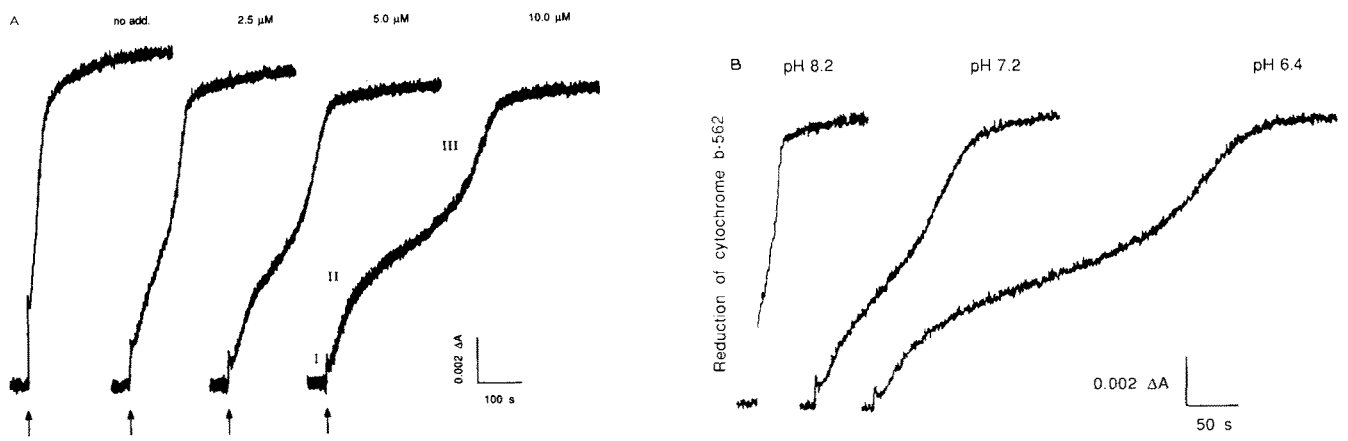

Fig. 5. (A) Time-course of reduction of cytochrome *b*-562 by DQH_2 in the presence of different amounts of Q_2 and absence of inhibitors of the bc_1 complex. pH 6.2. [KCN] = 1.0 mM. The Roman numbers refer to the distinct reduction phases (see text). (B) The effect of pH on the reduction of cytochrome *b*-562 by DQH_2 in the absence of inhibitors of the bc_1 complex. [Q_2] = 10 μM. [KCN] = 1.0 mM.

increasing pH. At pH 8.2, phases I and II (partially) overlap and the observed pattern of reduction of cytochrome *b*-562 is similar in uninhibited bc_1 complex and in the presence of myxothiazol (cf. Fig. 3B and Fig. 5B). However, in KCN-inhibited mitoplasts the degree (and kinetics) of the first phase of reduction of cytochrome *b*-562 is determined by the relative rates of oxidation of DQH_2 via the Q_{in}- and the Q_{out}-binding domains and by the equilibrium between cytochrome *b*-562 and the Q_2 pool via the Q_{in}-binding domain, whereas in the presence of myxothiazol all reactions via the Q_{out}-binding domain are inhibited.

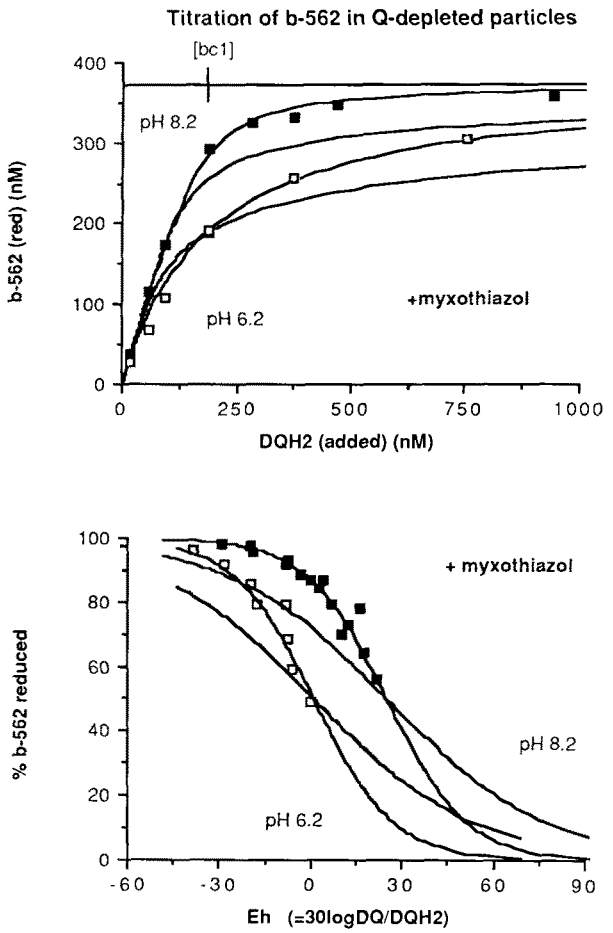

Fig. 6. Titration of cytochrome *b*-562 in the presence of myxothiazol with the DQH_2/DQ redox couple in Q-depleted particles at pH 6.2 (□) and pH 8.2 (■). The upper figure shows a direct plot of the concentration of cytochrome *b*-562 reduced (expressed in nM) versus the concentration of DQH_2 added. It is seen that for the titration performed at pH 8.2, but not for that at pH 6.2, all electrons of the DQH_2 added end up stoichiometrically in cytochrome *b*-562. The reason for this difference is that at pH 8.2 the value of E_m of cytochrome *b*-562 is 25 mV higher than that of the DQH_2/DQ couple, whereas at pH 6.2 they are similar (see lower figure). The lines through the points in the upper and lower figure are simulations of the Nernst equation with $n = 1$ and $n = 2$ and $E_m(b\text{-}562) = +1$ mV (relative to the $E_m(DQ/DQH_2)$) for pH 6.2 and +25 mV for pH 8.2. The data points conform to the $n = 2$ curves both at pH 6.2 and pH 8.2. [DQ] was determined as in Ref. 35.

Reduction of cytochrome b-562 by DQH_2 in Q-extracted preparations in the presence of myxothiazol

Fig. 6 shows that reduction of cytochrome *b*-562 by DQH_2 in Q-depleted particles inhibited by myxothiazol occurs with a single E_m, with $n_{app} = 2$ and that all electrons from DQH_2, taking into account the difference in E_m between cytochrome *b*-562 and DQH_2, are available for the reduction of cytochrome *b*-562. Furthermore, the E_m/pH dependency of the DQH_2/DQ couple is not the same as that of cytochrome *b*-562, i.e., at pH 6.2 both have the same E_m, but at pH 8.2 that of cytochrome *b*-562 is 25–30 mV higher (Fig. 6, lower panel).

Discussion

Enlarging the size of the Q pool by addition of Q_2 proves to be a valuable method for studying the redox behaviour of cytochrome *b* because it results in a high resolution of the different phases of reduction of cytochrome *b* without changing the main features of the pattern of reduction and, in addition, it offers the possibility to monitor the redox behaviour of both cytochrome *b* and the Q pool (i.e., Q_2) under the same experimental conditions.

Reduction of the Q pool and cytochrome b-562 by DQH_2 via the Q_{in}-reactive site

Using this method we have been able to show that in the presence of outside inhibitors the Q_{in}-reactive site as postulated in the Q cycle catalyzes the steady-state reduction of Q_2 (and Q_{10}, Ref. 15) by DQH_2 and that cytochrome *b*-562 rapidly equilibrates with the Q pool as evidenced by the traces shown in Fig. 2. The steady-state reduction of the Q pool by DQH_2 via the Q_{in}-reactive site is proposed to be the result of the following sequence of reactions (see also Ref. 27)

$$DQH_2 + E_{ox} \rightarrow DQ + E_{red} \quad (1)$$

$$Q + E_{red} \leftrightarrow E_{red}(Q) \quad (2)$$

$$E_{red}(Q) \leftrightarrow E_{ox} + QH_2 \quad (3)$$

$$DQH_2 + Q_2 \leftrightarrow DQ + Q_2H_2$$

i.e., the enzyme is reduced relatively slowly by DQH_2 and subsequently relatively rapidly oxidized by Q of the pool. The steady-state rate equation is derived in the Appendix and predicts that the initial rate of reduction of Q_2 shows saturation behaviour with respect to both DQH_2 and Q_2 and that the initial rate decreases with increasing concentrations of the product Q_2H_2, as observed. As to reaction 1, the finding that DQ is able to oxidize cytochrome *b*-562 (see Fig. 2) indicates that this reaction is not irreversible. However, the observation that addition of DQ has no effect on the rate of

reduction of the Q pool (not shown, but cf. Ref. 27) indicates that the reverse of reaction 1 does not occur at a kinetically competent rate, i.e., compared to the rate of reactions 2 and 3.

Reduction of cytochrome b-562 by DQH_2 in Q-depleted particles inhibited by myxothiazol

So far we have not specified the nature of the redox centers in the enzyme involved in reactions 1–3. Reaction 1 can be studied separately from reactions 2 and 3 in Q-extracted preparations (Fig. 6). It is observed that in Q-extracted preparations in the presence of an outside inhibitor DQH_2 reduces cytochrome *b*-562 to 95% without concomitant reduction of cytochrome *b*-566. Furthermore, cytochrome *b*-562 titrates with a single E_m, with $n_{app} = 2$ and, moreover, all electrons of DQH_2 end up in cytochrome *b*-562 (taking into account their respective differences in E_m).

In the following we will discuss how DQH_2 (a two-electron donor) might reduce cytochrome *b*-562 (a one-electron acceptor) stoichiometrically, with a single E_m and $n_{app} = 2$. Since oxygen is present during the titration of Fig. 6, the following sequence of reactions may occur:

$$DQH_2 + b^{3+} \rightarrow DQ^{\cdot -} + b^{2+} \quad (4)$$

$$DQ^{\cdot -} + O_2 \rightarrow DQ + O_2^{\cdot -} \quad (5)$$

which would result in a value of $n_{app} = 2$ and a single E_m for cytochrome *b*-562. However, in contrast to the observation, this sequence of reactions would imply that maximally half the number of electrons present in DQH_2 are available for the reduction of cytochrome *b*-562.

A possibility to reduce a one-electron acceptor stoichiometrically by a two-electron donor with a single E_m is when the two one-electron couples of the two electron donor have similar E_m values, in which case substantial amounts of the single electron intermediate are present. Due to the instability of $DQ^{\cdot -}$ this cannot be the case. Moreover, the one-electron acceptor would titrate with $n < 2$.

The mere fact that $DQ^{\cdot -}$ is a very unstable intermediate and that reduction of one cytochrome *b*-562 by DQH_2 yields $DQ^{\cdot -}$ implies that reduction of one cytochrome *b*-562 heme must be coupled tightly to the reduction of a second cytochrome *b*-562 heme. One way to accomplish this is when DQH_2 donates its two electrons in a concerted manner to two cytochrome *b*-562 hemes, i.e., DQH_2 is an obligate two-electron donor. This cannot, however, be the mechanism by which DQH_2 reduces cytochrome *b*-562, since first the two cytochrome *b*-562 hemes reside in different bc_1 monomers and, second, this would result in an $n = 1$.

A second way to accomplish this is when two molecules of DQH_2 bind to the $(D)Q_{in}$-binding sites of two bc_1 monomers each DQH_2 reducing a cytochrome *b*-562. The two molecules of $DQ^{\cdot -}$ thus formed will, subsequently, react with each other in a dismutation reaction. Thus, according to this alternative, the coupled reduction of the two cytochrome *b*-562 hemes by the two-electron donor DQH_2 requires the interaction of two bc_1 monomers at the level of $DQ^{\cdot -}$, specifically of $DQ^{\cdot -}$ bound at the Q_{in}-binding domain.

Previous studies indicate that QH_2:cytochrome *c* oxidoreductase is present in the membrane as a dimeric enzyme with each monomer containing one cytochrome *b* polypeptide carrying one heme *b*-562 and one heme *b*-566. Therefore, we propose that the coupled reduction of two cytochrome *b*-562 hemes by DQH_2 occurs via the interaction between the two protomers of the dimeric bc_1 complex and not via two (rapidly colliding) monomers. Also, the alternative of a direct movement of $DQ^{\cdot -}$ from one protomer to the other is, in our opinion, less likely, since $DQ^{\cdot -}$ is 'stable' (i.e. present at a kinetically competent concentration) for the very reason that it is *bound* to the Q-binding site.

Quantitative analysis of the equilibrium between cytochrome b-562 and the Q_2 pool in the presence of myxothiazol

We have indicated that, in the presence of myxothiazol, cytochrome *b*-562 is in rapid equilibrium with the Q_2 pool during the course of reduction of the Q_2 pool by DQH_2. From the traces of the course of reduction of the Q_2 pool and of cytochrome *b*-562, recorded separately but under identical experimental conditions, one can construct a graph in which the

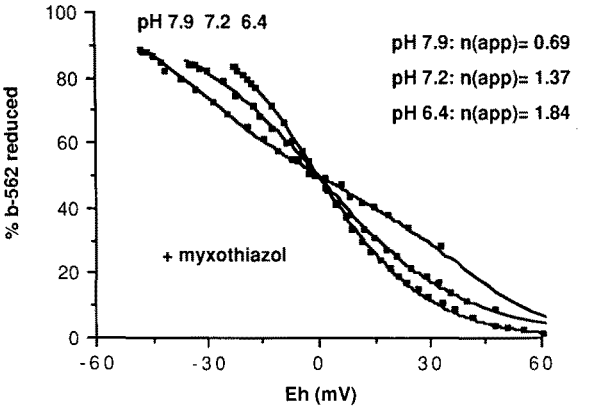

Fig. 7. Plot of percentage cytochrome *b*-562 reduced versus the redox potential (E_h). The redox state of cytochrome *b*-562 was determined from experimental traces as shown in Fig. 3B. The redox potential was calcualted as 30 $\log(Q_2/Q_2H_2)$. The $[Q_2H_2]$ was determined from experimental traces as in Fig. 3B. The E_h scale was normalized with respect to the E_m value of cytochrome *b*-562 (set arbitrarily at 0 mV for all pH values) since the E_m–pH dependency of cytochrome *b*-562 and the $(D)Q/(D)QH_2$ redox couples are different (see also Fig. 10). The lines through the experimental data points are simulations on basis of the model outlined in the text and the appendix. The values of *n*(app) were calculated from the simulations.

degree of reduction of cytochrome *b*-562 is plotted versus the ambient redox potential (calculated from the Q_2/Q_2H_2 ratio). This is shown in Fig. 7 for the myxothiazol inhibited enzyme. It is seen that the value of n_{app} (i.e., the slope at 50% reduction of cytochrome *b*-562) changes from close to 2 at low pH to values below 1 at pH 7.9. Thus at pH 6.4, cytochrome *b*-562 titrates with a single E_m ($n_{app} = 1.84$), whereas at pH 7.9 cytochrome *b*-562 titrates as two species with E_m values that differ by 50–100 mV, corresponding to the two forms of cytochrome *b*-562, called previously high- and low-potential cytochrome *b*-562 (cf. Refs. 8, 14, 17, 39, 40). Note that in Q-depleted particles cytochrome *b*-562 titrates with a single E_m and with $n_{app} = 2$ both at low and at high pH (Fig. 6) using DQH_2. In the following, we will develop a model in which a single type of cytochrome *b*-562 in equilibrium with the bound $Q_{in}^{\cdot-}$ (Q_{in}, $Q_{in}H_2$) is sufficient to explain qualitatively and quantitatively the redox behaviour of cytochrome *b*-562.

The characteristics of this model (Fig. 8) are as follows:

(A) The bc_1 complex is structurally dimeric.

(B) The two hemes *b*-562 reside in two different cytochrome *b* polypeptides located in the two protomers of the dimer.

(C) The two hemes *b*-562 have the same electrochemical properties, i.e., the same E_m.

(D) There is no direct electronic contact between the two hemes *b*-562.

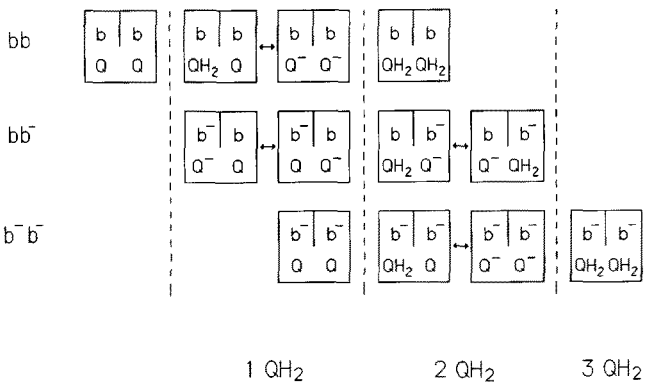

Fig. 8. Model of the equilibrium between cytochrome *b*-562 and the Q pool in the presence of outside inhibitors. b, b^-: oxidized and reduced cytochrome *b*-562. Q, Q^- and QH_2 represent the three intermediates of quinone bound to the Q_{in}-binding domain. The dimeric bc_1 complex is schematically drawn as a box showing only the two Q_{in}-binding domains, one in each protomer. Each protomer also contains one heme *b*-562. The 12 boxes represent the 12 possible redox states of the dimeric enzyme in the presence of an outside inhibitor, i.e., the enzyme can only accommodate an even number of electrons under these conditions, in contrast to the situation when mediators are present. Arrows connecting two boxes indicate single-electron transfer steps between two quinone species, analogous to electron transfer from Q_A to Q_B in photochemical reaction centers. See text for further details.

(E) In the vicinity of each heme *b*-562 a Q-binding domain exists in which the antimycin-sensitive $Q_{in}^{\cdot-}$ is stabilised.

(F) Electron transfer between heme *b*-562 and QH_2 ($Q_{in}^{\cdot-}$ and Q) bound to the Q_{in}-binding domain in the same protomer occurs unrestricted.

(G) Electron transfer between two quinones each present in one of the two Q_{in}-binding domains of the dimer takes place unrestricted in single electron transfer steps, thereby allowing the reactions:

$$(Q_{in}H_2)_1 + (Q_{in}^{\cdot-})_2 \leftrightarrow (Q_{in}^{\cdot-})_1 + (Q_{in}H_2)_2$$

$$(Q_{in})_1 + (Q_{in}^{\cdot-})_2 \leftrightarrow (Q_{in}^{\cdot-})_1 + (Q_{in})_2$$

$$(Q_{in})_1 + (Q_{in}H_2)_2 \leftrightarrow (Q_{in}^{\cdot-})_1 + (Q_{in}^{\cdot-})_2 \leftrightarrow (Q_{in}H_2)_1 + (Q_{in})_2$$

The combination of the reactions proposed in (F) and (G) allow electronic contact between the two hemes *b*-562 so that this one-electron redox couple may acquire the redox properties of a two-electron redox couple such as the quinone/quinol couple. Note that the middle of the reactions under (G) is similar to electron transfer from Q_A to Q_B that takes place in reaction centers.

(H) In the presence of an outside inhibitor, like myxothiazol the two Q_{in}-binding domains (including the two hemes *b*-562) can only accommodate an even number of electrons donated in the form of $(D)QH_2$. Consequently, the bc_1 complex may be present in any of the twelve different states shown in Fig. 8.

The redox behaviour of cytochrome *b*-562 can now be easily understood in terms of the model. Under conditions where no stable Q^- can be formed (e.g., at low pH) or DQ^- (at both low and high pH), the concentration of all intermediates containing a semiquinone (either one or two) is correspondingly low. As is clear from Fig. 8, the concentrations of the intermediates with one heme *b*-562 reduced are correspondingly low, indicating that the hemes *b*-562 in the dimer are both either reduced or oxidized, explaining values of *n* close to 2. Upon increasing the pH the stability of Q^- increases and the half-reduced state, containing a single Q^- and one heme *b*-562 reduced, becomes a prominent intermediate. In this case, cytochrome *b*-562 shows electrochemical behaviour similar to that of the quinones, i.e., reduction takes place in two distinct steps (cf. Fig. 7). Finally, the model predicts that at very high stability of Q^- ($K_{stab} > 10$), cytochrome *b*-562 would again titrate with $n = 2$, since now the intermediates containing two Q^- are the most prominent ones, the half-reduced states being present in much lower concentration. Such a high stability of $Q_{in}^{\cdot-}$ is, however, not observed experimentally [41–43] (see also Fig. 10).

In the Appendix, the method to simulate the experimental traces of reduction of the Q_2 pool and cyto-

chrome *b*-562 on basis of this model is outlined in detail. The only parameter that was varied to simulate the redox behaviour of cytochrome *b*-562 at the different pH levels (Figs. 7 and 9) was the stability of $Q_{in}^{\cdot-}$ (expressed as the difference between E_1 (E_m $Q_{in}^{\cdot-}/QH_2$) and E_2 (E_m $Q/Q_{in}^{\cdot-}$)), since the relative E_m values of cytochrome *b*-562, the DQH_2/DQ and the QH_2/Q redox couples were determined essentially independently (cf. Fig. 6 and Appendix). Fig. 10 shows the E_m-pH dependency of the various components. As noted previously from titrations with the fumarate/succinate redox couple, the E_m of cytochrome *b*-562 varies by only 40–45 mV/pH [8]. It is also seen that the E_m values of the two one-electron quinone couples determined by simulation of the kinetics of reduction of cytochrome *b*-562 vary in the same manner as observed previously in potentiometric titrations of the antimycin-sensitive $Q_{in}^{\cdot-}$, i.e., below pH 7.6 E_1 and E_2 have slopes of −120 and 0 mV/pH, respectively, above pH 7.6 both slopes become −60 mV/pH (Refs. 41, 42 and see Ref. 43 for the interpretation of this pK). The finding that the same pH dependency for E_1 and E_2 is found by two independent methods indicates that the

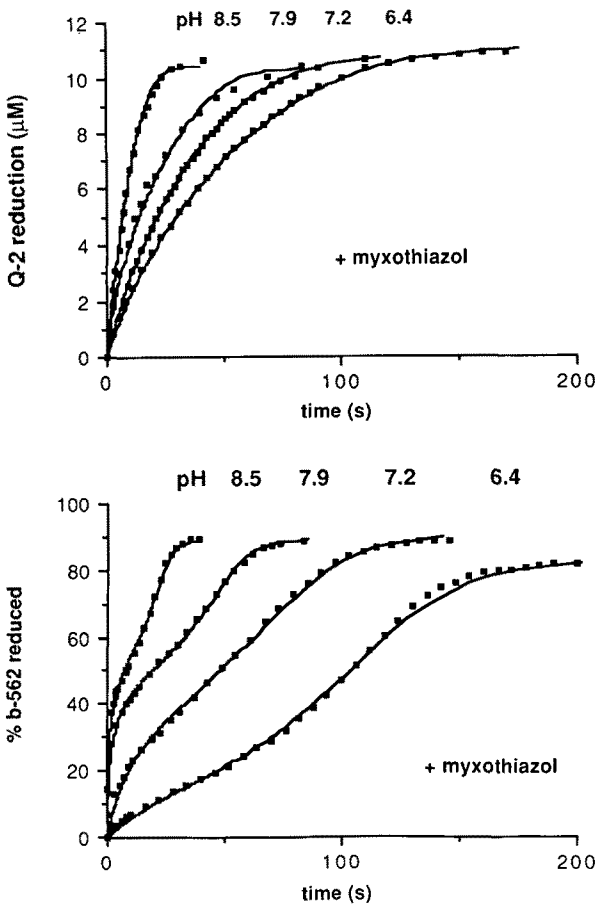

Fig. 9. Simulation of the experimental traces (digitized) of Q_2 and cytochrome *b*-562 reduction in the presence of myxothiazol recorded at the indicated pH values. The simulation parameters are given in Table I of the appendix. See text for further details.

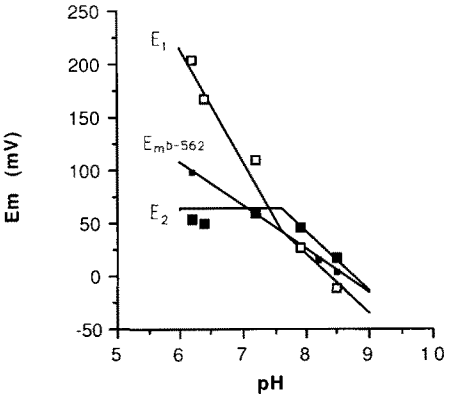

Fig. 10. The E_m–pH dependency of cytochrome *b*-562 (E_m*b*-562), the $Q^{\cdot-}/QH_2$ (E_1) and the $Q/Q^{\cdot-}$ (E_2) redox couples as determined by simulation of the experimental traces of cytochrome *b*-562 reduction in the presence of myxothiazol (cf. Figs. 3B and 9 and Table I of the Appendix). The line through the points of E_m*b*-562 has a slope of −41 mV/pH (at 2–3°C $RT/F = 55$ mV). The data points of E_1 and E_2 are fitted with slopes of −110 and 0 mV/pH, respectively, below pH 7.6 and above pH 7.6 the slope for both equals −55 mV/pH. See text for further details.

redox behaviour of cytochrome *b*-562, in particular the multiphasic pattern of reduction, is very strongly determined by the properties of quinone bound to the Q_{in}-binding domain, in particular by the stability of the antimycin-sensitive $Q_{in}^{\cdot-}$.

Figs. 7 and 9 indicate that the fit to the experimental traces is satisfactory. However, to simulate the redox behaviour of cytochrome *b*-562 at pH 7.9 and pH 8.5 optimally, an additional assumption had to be made. Either the (relative) concentration of the intermediates containing two semiquinones are strongly reduced (the value of *b* approaches zero in Eqn. 5 of the Appendix) or the intermediates containing one semiquinone are present at a concentration 2-times higher than calculated in Eqn. 5 (see Appendix), i.e., the factor 4 bcomes 8. In either case, the fit was satisfactory (cf. Figs. 7 and 9). With either of these assumptions the simulations of the traces recorded at lower pH values are hardly affected for the sole reason that the concentration of semiquinone at low pH is insignificant. Of the two possibilities mentioned above to optimize the simulation of the reduction of cytochrome *b*-562 we favour selective destabilization of intermediates containing two $Q_{in}^{\cdot-}$ radicals, since it results in maximum values of $Q_{in}^{\cdot-}$ per bc_1 complex of about 0.5, as found experimentally [42,43]. Destabilization might be due to an unfavourable electrostatic interaction between the two semiquinones, resulting in dismutation. In fact, the break in the E_m/pH curves at pH 7.6 of E_1 and E_2 observed in this work and in equilibrium potentiometric titrations might even be a reflection of such an interaction. Destabilization might also be of physiological relevance, since under conditions that the semiquinone is very stable, the step from semiquinone to quinol becomes thermo-

dynamically very unfavourable, preventing oxidation of cytochrome *b*-562 and as a consequence inhibiting turnover.

Reduction of the Q pool and cytochrome b-562 in the absence of bc_1 inhibitors: a reevaluation

In the presence of KCN, but in the absence of cytochrome bc_1 inhibitors, DQH_2 may reduce the enzyme via both the Q_{out}- and the Q_{in}-binding domains, resulting in initial rapid reduction of part of cytochrome *b*-562 and Q (the latter cannot be resolved under our experimental conditions, but see the results of Ref. 15 in which is shown that $1Q/bc_1$ is rapidly reduced). However, once cytochrome c_1 and the Rieske Fe-S cluster are completely reduced (which takes about 1.5 s in our experiments) reduction of the Q pool can proceed only via the Q_{in}-reactive domain. Nevertheless, the pattern of reduction of cytochrome *b*-562 in BAL-inhibited and uninhibited enzymes are not the same after the first few seconds (cf. Figs. 2 and 5A). This can be explained as follows. In the presence of an outside inhibitor the Q_{in}-binding domain can accommodate only an even number of electrons. In the absence of inhibitors, full reduction of cytochrome c_1 and the Rieske Fe-S cluster requires the oxidation of 2 molecules of DQH_2 by the Q_{out}-binding domain, yielding two electrons in the Q_{in}-binding domain, i.e., an even number. However, in mitoplasts inhibited by KCN electrons on cytochrome c_1 and the Rieske Fe-S cluster will equilibrate via (residual) cytochrome *c* with cytochrome *c* oxidase. Clearly, it depends on the amount of the latter two compared to the amount of the bc_1 complex whether an even or odd number of molecules of DQH_2 is oxidized in order to reduce the high-potential part of the respiratory chain (in addition, there is always a small leak through the KCN block). Thus, apart from the intermediates depicted in Fig. 8, intermediates having an odd number of electrons in the Q_{in}-binding domain may also be present in the KCN-inhibited mitoplasts. In this case, the equilibrium between cytochrome *b*-562 and the Q_2 pool may be described by a simple ($n = 1$) Nernst curve. In fact, at pH 6.4 the value of n_{app} for the reduction of cytochrome *b*-562 equals 1.17 for the KCN-inhibited mitoplasts and for the BAL-inhibited mitoplasts $n_{app} = 1.98$ (cf. Figs. 2 and 5A).

The initial rapid reduction of cytochrome *b*-562 by DQH_2 has previously been ascribed to reduction via the Q_{in}-reactive site [14,17]. However, experiments performed in the presence of a large Q pool show that outside inhibitors abolish the initial rapid reduction phase which is best seen at low pH. We therefore conclude that the initial rapid reduction of cytochrome *b*-562 (the 5 ms phase) observed in the absence of inhibitors is due to the arrival of reducing equivalents produced by the oxidation of DQH_2 at both the outside and inside, the relative contribution of each route being dependent on the specific experimental conditions, e.g., the capacity of the high-potential part of the respiratory chain and the size of the Q pool. Inspection of the original traces of the pre-steady state kinetics of reduction of the prosthetic groups in the absence of inhibitors (see Fig. 1 of Ref. 17) shows that the amount of electrons present in the Fe-S cluster and cytochrome c_1 after 5 ms is sufficient to account for the extent (30–40%, pH 6.6–9.3) of reduction of cytochrome *b*-562, this in spite of the fact that the $t_{1/2}$ of reduction of the Fe-S cluster and cytochrome c_1 are about 15 ms. In experiments in which succinate is used as reductant [10–13] the initial rapid reduction of cytochrome *b*-562 occurs via the Q_{out}-binding domain because, initially, the redox potential of the Q pool is too high to cause substantial reduction of cytochrome *b*-562 via the Q_{in}-binding domain.

Reduction of the Q pool and cytochrome b by DQH_2 via the Q_{out}-reactive site

The traces of Fig. 4 show that in the presence of antimycin a steady-state reduction of the Q_2 pool by DQH_2 occurs. Since this reaction is inhibited by myxothiazol, reduction of the Q pool takes place via the Q_{out}-reactive site. The rate of the reaction is dependent on the redox state of the Rieske 2Fe-2S cluster, which was manipulated by the addition of cytochrome *c*. The maximal rate observed was approximately equal to that obtained in KCN-inhibited preparations (cf. Fig. 4).

Although the reduction of cytochrome *b* in the presence of antimycin is normally monophasic [11,17,18], enlarging the size of the Q pool leads to a biphasic reduction pattern. In the first phase, cytochrome *b*-562 becomes reduced and when the Q pool is reduced to a great extent, cytochrome *b*-566 becomes reduced. The reduction of the Q pool via the Q_{out}-binding site is proposed to proceed according to the following (cytochrome *b*-562 is already reduced):

$$DQH_2 + [b^{3+}_{566}\text{--(Fe-S)}] \rightarrow DQ + [b^{2+}_{566}\text{--(Fe-S)}^-]$$

$$[b^{2+}_{566}\text{--(Fe-S)}^-] + Q \leftrightarrow [b^{3+}_{566}\text{--(Fe-S)}] + QH_2$$

in which binding and dissociation of Q and QH_2 are omitted. From these reactions it is clear that reduction of the Q_2 pool by DQH_2 will not occur when the Fe-S cluster is kept either fully oxidized or fully reduced (cf. Fig. 4) and that the maximal rate will occur at an intermediate redox state. Furthermore, the equilibrium between the two-electron pair [b_{566}--(Fe-S)] and the Q_2 pool can be sustained by a single protomer, in contrast to the equilibrium between cytochrome *b*-562 and the Q_2 pool.

In this paper we have shown that the steady-state reduction of Q_2 by DQH_2 may be catalysed by the Q_{in}-binding domain in cooperation with cytochrome

b-562 and by the Q_{out}-binding domain in which case cytochrome *b*-566 and the Rieske Fe-S cluster are involved. We have analysed quantitatively the equilibrium between cytochrome *b*-562 and the Q_2 pool, in the presence of myxothiazol, and concluded that there exists a pathway of electron transfer between two Q_{in}-binding domains allowing redox equilibration, in single electron-transfer steps, between the two hemes *b*-562 of the dimeric bc_1 complex. In our initial attempts to simulate this equilibrium in terms of a monomeric bc_1 complex we found that such a system may produce the multiphasic pattern of reduction of cytochrome *b*, but that the simulations did not fit the experimental traces satisfactorily. Furthermore, it was noticed that substantial amounts of cytochrome *b*-566 should become reduced, especially in the second reduction phase (see, for example, the simulation in Fig. 4 of the paper by West [13]), but since this is not observed experimentally we turned to a description of the equilibrium in terms of a dimeric bc_1 complex. The scheme of Fig. 8 should, however, not be considered to rule out the possibility that initially the two electrons of DQH_2 are distributed between cytochrome *b*-562 and cytochrome *b*-566. However, since no *net* reduction of cytochrome *b*-566 is observed experimentally, this cytochrome may only be transiently reduced. Consequently, transient reduction of cytochrome *b*-566, in combination with the finding that, in the presence of myxothiazol, both electrons of DQH_2 end up in cytochrome *b*-562 (with the value of $n_{app} = 2$), indicates that any electron residing on cytochrome *b*-566 should be rapidly donated to cytochrome *b*-562 and the electron initially present on this latter cytochrome should be rapidly donated to (D)Q. The $(D)Q^-$ thus formed rapidly reduces a second cytochrome *b*-562. Also in this variant, a pathway allowing rapid equilibration between two hemes *b*-562 via the Q_{in}-binding domains should exist. Fig. 8 shows this pathway.

Lack of reduction of cytochrome *b*-566 as reported here is in part due to the low $[DQH_2]$ used, since in kinetic experiments (in Q-depleted particles) employing much higher concentrations of DQH_2, cytochrome *b*-566 becomes reduced after initial reduction of cytochrome *b*-562 [17]. Furthermore, because cytochrome *b*-562 (and possibly cytochrome *b*-566) titrates with $n_{app} = 2$, the reduction phases of the two cytochromes *b* are much more separated in the experiment of Fig. 6 than in potentiometric titrations in the presence of mediators.

In the work of Chen and Zhu [12], the equilibrium between cytochrome *b*-562 and the Q_2 pool was studied using succinate as reductant. In order to describe the multiphasic pattern of reduction of cytochrome *b*-562, these authors assumed the presence of two cytochromes *b*-562 with different redox midpoint potentials. We have shown in the simulations that such an assumption is not required. Monophasic or multiphasic reduction of cytochrome *b*-562 in the presence of myxothiazol, is, to a great extent, determined by the stability of the antimycin-sensitive $Q_{in}^{\cdot -}$. According to Salerno et al. [44], however, the stability of the semiquinone is not high enough to give rise to a biphasic reduction pattern of cytochrome *b*-562. The simulation of the kinetics of reduction of cytochrome *b*-562 on basis of the model of Fig. 8 indicates, however, that the best fits are obtained either by selectively stabilizing intermediates containing a single $Q_{in}^{\cdot -}$, i.e., in line with Salerno's suggestion, or by selectively destabilizing intermediates containing two species of $Q_{in}^{\cdot -}$, the possibility we favour.

It is likely that, in order to refine the quantitative description of the equilibrium between cytochrome *b*-562 and the Q-pool, interactions between semiquinone(s) and cytochrome *b*-562 should be taken into account as well as differential binding affinities for Q and QH_2 and the various protonation states of QH_2. This is currently under investigation.

Acknowledgements

We thank Drs. E.C. Slater and J.A. Berden for their interest and stimulating discussions, Dr. Hoffle for the gift of stigmatellin and Mr. A.F. Hartog for preparing Q_2. S.d.V. thanks the Royal Dutch Academy of Sciences (KNAW) for a fellowship.

Appendix

Procedure to simulate the time-course of reduction of Q_2 and cytochrome b-562

The simulation procedure consists of two steps:
(1) The time-course of reduction of Q_2 is simulated from which the change in redox potential in time was calculated from the Q/QH_2 ratio.
(2) The degree of reduction of cytochrome *b*-562 as a function of the redox potential determined from the simulation of the Q-reduction traces, was calculated using the model depicted in Fig. 8.

(1) Steady-state reduction of Q_2 is described by the equations

$$DQH_2 + E_{ox} \leftrightarrow DQ + E_{red} \qquad K_1 = k_1/k_{-1}$$

$$E_{red} + Q \leftrightarrow E_{red}(Q) \qquad K_2 = k_2/k_{-2}$$

$$E_{red}(Q) \leftrightarrow E_{ox} + QH_2 \qquad K_3 = k_3/k_{-3}$$

The steady-state rate equation becomes [45]:

$$\begin{aligned} v/e &= -1/e \cdot dQ/dt \\ &= \{k_1k_2k_3DQH_2 \cdot Q - k_{-1}k_{-2}k_{-3}DQ \cdot QH_2\} \\ &\quad / \{k_{-1}DQ(k_{-2}+k_3) + k_2k_3Q + k_1DQH_2(k_{-2}+k_3) \\ &\quad + k_{-2}k_{-3}QH_2 + k_{-1}k_{-3}DQ \cdot QH_2 + k_1k_2DQH_2 \cdot Q \\ &\quad + k_2k_{-3}Q \cdot QH_2\} \end{aligned}$$

TABLE I

Kinetic and thermodynamic constants for the equilibrium between Q_2 and cytochrome b-562 determined from the time course of reduction.

pH	Parameters used to simulate the rate of Q_2 reduction						Parameters of the Q–*b* equilibrium [a]		
	k_1 ($M^{-1}\,s^{-1}$)	k_{-1} ($M^{-1}\,s^{-1}$)	k_2 ($M^{-1}\,s^{-1}$)	k_{-2} (s^{-1})	k_3 (s^{-1})	k_{-3} ($M^{-1}\,s^{-1}$)	E_1 (mV)	E_2 (mV)	$E_m b$ (mV)
6.2	$1.1\cdot10^5$	$1.1\cdot10^5$	$1.4\cdot10^6$	0.32	10.3	$4.5\cdot10^6$	204	54	99
6.4	$1.1\cdot10^5$	$1.1\cdot10^5$	$1.4\cdot10^6$	0.32	10.3	$4.5\cdot10^6$	168	50	98
7.2	$3.0\cdot10^5$	$1.1\cdot10^5$	$1.4\cdot10^6$	0.52	10.3	$7.5\cdot10^6$	110	59	59
7.9	$6.7\cdot10^5$	$1.1\cdot10^5$	$6.0\cdot10^6$	2.09	20	$3.5\cdot10^7$	26	46	29
8.5	$1.1\cdot10^6$	$1.7\cdot10^5$	$1.0\cdot10^7$	2.57	25	$6.3\cdot10^7$	−12	18	3

[a] These values are plotted in Fig. 10.

This equation was time-integrated according to Ref. 46 and used to simulate the Q-reduction traces.

(2) The degree of reduction of cytochrome *b*-562 in the presence of an outside inhibitor as function of the redox potential and assuming that the standard midpoint potentials of bound and free Q_2 are the same is given by the equation:

$$\frac{b^{2+}\text{-}562}{\text{dimer}} = \frac{4\cdot\sqrt{b}\cdot\sqrt{c}\,(1+a)+2\cdot c\,\{(1+a)^2+b\}}{4\cdot\sqrt{b}\cdot\sqrt{c}\,(1+a)+(1+c)\cdot\{(1+a)^2+b\}}$$

in which $a = 10^{(E_Q - E_h)/30}$, $b = 10^{(E_2 - E_h)/30}$ with $E_2 = E_m(Q/Q^-)$ and $c = 10^{(E_{b\text{-}562} - E_h)/30}$.

Determination of the simulation parameters (cf. Table I)

All standard midpoint potentials are determined or calculated relative to that of the DQ/DQH_2 redox couple with $E_{m7} = 55$ mV [47]. The standard midpoint potential of cytochrome *b*-562 was determined in Q-free particles at different pH values (as in Fig. 6) and in Q-containing particles form the level of reduction obtained at various DQ/DQH_2 ratios. The values from Q-depleted and Q-containing particles differed by no more than 5–10 mV. The E_{m7} $(Q_2/Q_2H_2) = 85$ mV was determined experimentally by monitoring the redox state of cytochrome *b*-562 in the presence of different ratios of Q_2/Q_2H_2 (and/or DQ/DQH_2). Values for k_1 were determined from the rate of reduction of cytochrome *b*-562 by DQH_2 in Q-free particles (in the presence and absence of inhibitors). The value of k_{-1} was calculated from the midpoint potential of cytochrome *b*-562 and k_1. The values of k_2, k_3 and k_{-3} were estimated from traces as shown in Fig. 1. Knowing these constants, the value of k_{-2} can be calculated and the experimental trace of the reduction of the Q_2 pool was fitted. In order to optimize the fit of the traces of reduction of the Q_2 pool the values of k_2, k_3 and k_{-3} were varied. After fitting the Q_2-reduction traces, the traces of the reduction of cytochrome *b*-562 in the presence of myxothiazol were simulated by varying E_1 ($E_m(Q^-/QH_2)$ and E_2 ($E_m(Q/Q^-)$. In order to fit the course of reduction of cytochrome *b*-562 at pH 7.9 and 8.5, the expression for reduced *b*-562/dimer could be changed by replacing the factor of 4 to 8 (i.e., selective stabilization of the intermediates containing a single semiquinone) or by omitting the term *b* (in both nominator and denominator), i.e., selective destabilization of the intermediates containing two semiquinones (see Discussion for further details).

References

1 Kröger, A. and Klingenberg, M. (1973) Eur. J. Biochem. 34, 358–368.
2 Kröger, A. and Klingenberg, M. (1973) Eur. J. Biochem. 39, 313–323.
3 Mitchell, P. (1976) J. Theor. Biol. 62, 327–367.
4 Crofts, A.R. and Wraight, C.A. (1983) Biochim. Biophys. Acta 726, 149–186.
5 Hauska, G., Hurt, E., Gabellini, N. and Lockau, W. (1983) Biochim. Biophys. Acta 726, 97–133.
6 Rich, P.R. (1984) Biochim. Biophys. Acta 768, 53–79.
7 Wikström, M. and Krab, K. (1986) J. Bioenerg. Biomembr. Vol. 18, 181–193.
8 De Vries, S. (1986) J. Bioenerg. Biomembr. 18, 195–224.
9 Crofts, A.R. (1986) J. Bioenerg. Biomembr. 18, 437–445.
10 Jin, Y.Z., Tang, H.L., Li, S.L. and Tsou, C.L. (1981) Biochim. Biophys. Acta 637, 551–554.
11 Tang, H.L. and Trumpower, B.L. (1986) J. Biol. Chem. 261, 6209–6215.
12 Chen, M. and Zhu, Q.S. (1986) Biochim. Biophys. Acta 851, 457–468.
13 West, I.C. (1989) Biochim. Biophys. Acta 976, 182–189.
14 De Vries, S., Albracht, S.P.J., Berden, J.A. and Slater, E.C. (1982) Biochim. Biophys. Acta 681, 41–53.
15 Van Hoek, A.N., Van Gaalen, M.C.M., De Vries, S. and Berden, J.A. (1987) Biochim. Biophys. Acta 892, 152–161.
16 Matsuura, K. and Dutton, P.L. (1981) in Chemiosmotic Proton Circuits in Biological Membranes (Skulachev, V.P. and Hinkle, P., eds.), pp. 259–270, Addison-Wesley, Reading, MA.
17 De Vries, S., Albracht, S.P.J., Berden, J.A., Marres, C.A.M. and Slater, E.C. (1983) Biochim. Biophys. Acta 723, 91–103.
18 Meinhardt, S.W. and Crofts, A.R. (1983) Biochim. Biophys. Acta 723, 219–230.
19 Glaser, E.G., Meinhardt, S.W. and Crofts, A.R. (1984) FEBS Lett. 178, 336–342.
20 Robertson, D.E., Giangiacomo, K.M., De Vries, S., Moser, C.C. and Dutton, P.L. (1984) FEBS Lett. 178, 343–349.
21 Joliot, P. and Joliot, A. (1986) Biochim. Biophys. Acta 849, 211–222.

22 Rich, P.R., Heathcote, P. and Moss, D.A. (1987) Biochim. Biophys. Acta 892, 138–151.
23 Venturoli, G., Fernandez-Velasco, J.G., Crofts, A.R. and Melandri, B.A. (1988) Biochim. Biophys. Acta 935, 258–272.
24 Marres, C.A.M. and Berden, J.A. (1984) EBEC Rep. 2, 147–148.
25 De Vries, S. and Marres, C.A.M. (1985) in Proton pumping in respiration and photosynthesis, pp. 46–48, Table Ronde Rousel-Uclaf, No. 52, Paris.
26 Linke, P., Bechmann, G. and Weiss, H. (1986) Eur. J. Biochem. 158, 615–622.
27 Zweck, A., Bechmann, G. and Weiss, H. (1989) Eur. J. Biochem. 183, 199–203.
28 Tsou, C.L. (1952) Biochem. J. 50, 493–499.
29 Norling, B., Glazek, E., Nelson, B.D. and Ernster, L. (1974) Eur. J. Biochem. 47, 475–482.
30 Slater, E.C. (1949) Biochem. J. 45, 14–30.
31 Sugihane, H., Watanabe, M., Kawamatsu and Morimoto, H. (1972) Lieb. Ann. Chem. 763, 109–120.
32 Strong, F.M., Dickie, J.P., Loomans, M.E., Van Tamelen, E.E. and Dewey, R.S. (1960) J. Am. Chem. Soc. 82, 1513–1515.
33 Thierbach, G. and Reichenbach, H. (1981) Biochim. Biophys. Acta 638, 282–289.
34 Thierbach, G., Kunze, B., Reichenbach, H. and Hoffle, G. (1984) Biochim. Biophys. Acta 765, 227–235.
35 Van Ark, G. (1980) Electron transfer through the ubiquinol: ferricytochrome *c* oxidoreductase segment of the mitochondrial respiratory chain, Ph.D. Thesis, University of Amsterdam, Rodopi, Amsterdam.
36 Berden, J.A. and Slater, E.C. (1972) Biochim. Biophys. Acta 256, 199–215.
37 Zaugg, W.S. and Rieske, J.S. (1962) Biochem. Biophys. Res. Commun. 9, 213–220.
38 Berden, J.A. (1972) in Site II of the respiratory chain, Ph.D. Thesis, University of Amsterdam, Gerja-Drukkerij, Waarland.
39 Berden, J.A. and Opperdoes, F.R. (1972) Biochim. Biophys. Acta 267, 7–14.
40 Wikström, M.K.F. (1973) Biochim. Biophys. Acta 301, 155–193.
41 Ohnishi, T. and Trumpower, B.L. (1980) J. Biol. Chem. 255, 3278–3284.
42 De Vries, S., Berden, J.A. and Slater, E.C. (1980) FEBS Lett. 122, 143–147.
43 Robertson, D.E., Prince, R.C., Bowyer, J.R., Matsuura, K., Dutton, P.L. and Ohnishi, T. (1984) J. Biol. Chem. 259, 1758–1763.
44 Salerno, J.C., Xu, Y., Osgood, M.P., Kim, C.H. and King, T.E. (1989) J. Biol. Chem. 264, 15398–15403.
45 Cleland, W.W. (1963) Biochim. Biophys. Acta 67, 104–137.
46 Darvey, I.G. and Williams, J.F. (1964) Biochim. Biophys. Acta 85, 1–10.
47 Clark, W.M. (1960) in Oxidation-Reduction Potentials of Organic Systems, Waverly Press, Baltimore.